AC 2008-298: A BALLISTIC MISSILE SEARCH AND TRACKING SYSTEM

Charles Bittle, University of North Texas

Mitty Plummer, University of North Texas

CHARLES C. BITTLE has been a Lecturer at the University of North Texas since 1997. He earned his B.S.E.E. at Lamar State School of Technology in 1960 and his M.S.E.T. at the University of North Texas in 2000. Mr. Bittle served in the U.S. Federal Service for 32 years.

MITTY C. PLUMMER is an associate professor at the University of North Texas since 1992. He earned his BSEE, MENE, and PhD from Texas A&M. He worked in a variety of industrial positions for 22 years before joining UNT.

A Ballistic Missile Beacon Search and Tracking System

Introduction

The College of Engineering at this university will offer a new Mechatronics Engineering Degree during the fall semester of 2008. The curriculum for this degree has been approved. Authors of this paper are proposing an elective course be developed for Mechatronics students covering missile defense technology. The curriculum for the course should cover systems needed for a ballistic missile defense engagement during powered, ballistic, and re-entry flights. The search, tracking and targeting systems will be different for powered, ballistic, and re-entry flight paths of the missile. The course should start with the powered flight part of the missiles trajectory. This paper would fit within the powered flight part of the course. Much work is needed to develop the total curriculum of the course. In addition, a text book for the course should be written to include the design of all the subsystems needed for these engagements.

In the early 1970's, the first author was evolved with designing, building and installing successful ground based missile search and tracking systems for the Department of Defense. Funds for additional ground based missile search and tracking systems were not allocated because a decision was made to deploy satellite missile defense systems. The 1972 Antiballistic Missile (ABM) Treaty with the Soviet Union delayed development of missile defense systems by the United States (U.S.). This treaty created a scenario where a hostile country launches missiles at the U.S. and the U.S. retaliates by launching its missiles at the hostile country. Now, the U.S. has a National Missile Defense (NMD) program that is developing missile defense systems. The most pressing concern today is the feasibility of an attack by North Korean or Iranian ballistic missiles bearing nuclear or biological weapons. Hypothesizing that a North Korean or Iranian missile destroys a city like San Francisco or New York in the future, NMD program will become the highest priority program for the U.S. In January 2008, American Airlines announced that they were starting a missile defense program to protect their airplanes.

Universities should start teaching missile defense technology now to expose engineering students to missile defense. A Mechatronics (Mechanical / Electronics) program would be a good place to offer a course covering missile defense technology since missile defense systems contain predominately mechanical / electronics systems.

The proposed missile defense (MD) engineering course could be an exciting course in which the student could apply his/her engineering talents. The missile search and tracking system described in this paper will provide an example of the diversity required of the student. It goes through a design process that is representative of a system that must be analyzed, designed and tested. It is an example of how a system transfer

function is found by developing each component's transfer function (see Appendix 1). It will be only a part of the course and will need the student to interact with colleagues in mechanical, electrical and computer engineering, not to mention mathematics and physics. After completing the MD course, the student will see how previous courses fit into the large picture of system design.

The student will learn that the advent of missile test launches by foreign countries and absents of tracking information required for radar systems led to the need for a beacon search and tracking system. This paper describes the design of such a system. The system has two-closed loop subsystems and two modes of operation: search and automatic tracking. These subsystems are analyzed mathematically and subsystem characteristics are determined by using MATLAB's SIMULINK software package. Scientific Notebook software was used to develop and solve equations included in this paper. The location of the search and tracking system is referred to as the observation site in this paper

Large radar systems have a difficult time accomplishing a window search pattern on the horizon to locate foreign missiles. The momentum of an 80-foot diameter radar dish can cause expensive damage to the system drive gears when changing directions during a window search. A smaller and faster 6-foot beacon search and tracking system will complement the larger radar system. Figure 1 shows the antenna pedestal with search and tracking antennas mounted on the pedestal.

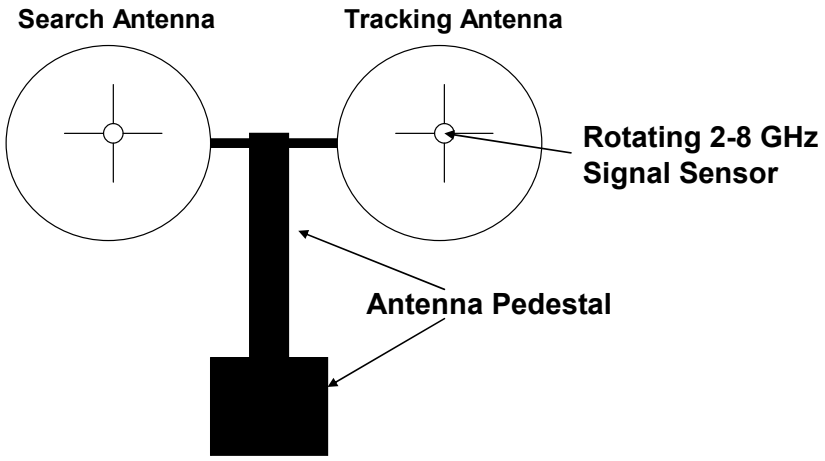

Figure 1 Antenna Pedestal

From a military point of view, a ballistic missile has the sole objective of carrying an explosive warhead from the launch point to the impact point or target. Both points are on the trajectory plane and surface of the Earth. A typical trajectory of a ballistic missile

is shown in Figure 2. The trajectory is divided into powered, ballistic, and re-entry flights. During powered flight, the missile goes from a static position to dynamic flight and is propelled beyond the appreciable atmosphere. A propulsion system accelerates the missile to a velocity where it will enter ballistic flight, a predetermined flight path beyond the appreciable atmosphere. The missile moves along without further expenditure of energy until it re-enters the atmosphere near the impact point.[1] Location of the search and tracking system is referred to as the observation point in this paper. The observation point is shown in Figure 2. The center line or zero azimuth of the antenna pedestal always points to the North Pole.

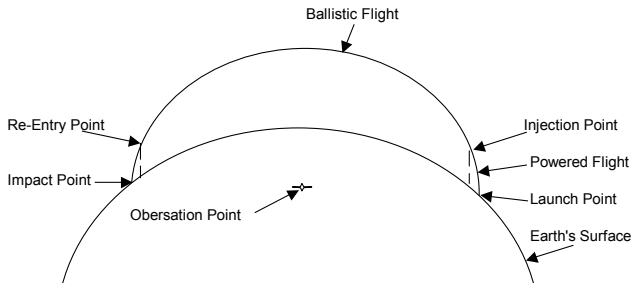

Figure 2 Typical trajectory of a ballistic missile

A search subsystem is needed to detect the launch of one or more ballistic missiles to provide early warning. The missile's on-board tracking beacon is of primary interest to a missile defense system. A beacon tracking system is used at the launch site to track and keep the missile on the proper flight path during powered flight. During the 1970's, beacon signals were in the 2-6 Giga Hertz (GHz) frequency range. A ground based 2-6 GHz signal will normally propagate straight off the earth. However, experience has shown the signal will bend over the horizon during the missile's powered flight. The search subsystem at the missile defense site will detect the beacon signal before the missile breaks the horizon to be acquired by radar. The tracking subsystem at the observation point could be already locked on to the missile's tracking beacon and providing early warning of the missile launch prior to the missile's horizon break point. The tracking radar subsystem could operate in synchronism with the bacon tracking system and take over tracking the missile at the horizon break point. Also, the targeting system could be calculating the antimissile intercept point before the missile breaks the horizon. In this scenario, the missile could be destroyed in powered flight or just when it enters ballistic flight. A search window around the point where the missile is predicted to break the horizon will allow the beacon tracking system to locate the beacon signal.[2]

System Operation

The search mode is initiated by an operator entering the latitude and longitude of the launch, impact and observation point locations into the system computer. The computer program (not included in this paper) calculates the horizon break of the missile[2]. A computer program drives the antenna to the horizon break point and

initiates a window search about that point. The tracking subsystem is always providing signal strength to the 2-8 GHz receiver and angle of rotation of the signal sensor, shown in Figure 1, to another computer program (not included in this paper). An operator monitors the receiver display and switches to the auto-track mode when the beacon signal is detected. In the auto-track mode, a computer program uses the automatic gain control voltage of the receiver and signal sensor angle to calculate the azimuth and elevation drive voltage necessary to drive the antenna along with the missile. The radar system operator is monitoring the azimuth and elevation displays of the tracking subsystem. When the beacon tracking system switches to the auto-track mode, the radar operator drives the radar antenna to the azimuth and elevation values shown on these displays.

Search Subsystem

The azimuth position control system converts position inputs from the computer to position output responses that drive the antenna in both azimuth and elevation. The azimuth and elevation position control systems are identical except they receive different position inputs. Thus, only the azimuth position control system will be discussed in detail. The block diagram of the azimuth position control system is shown in Figure 2.

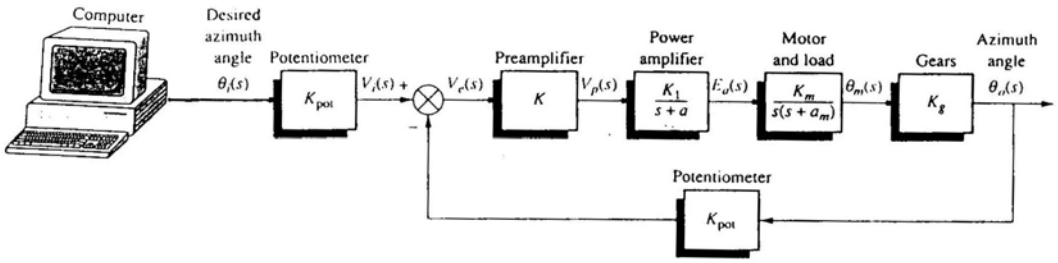

Figure 2 Block diagram of the azimuth position control system.

The system normally operates to drive the error to zero. When the input and output match, the error will be zero and the drive motor will not turn. Thus, the motor is driven only when the output and the input do not match. The difference between input and output voltage determines how fast the motor will turn. The larger the difference voltage, the faster the motor turns. The difference in response will cause transients if the motor amplifier gain is two large. Since the motor drives harder at higher voltages, it turns faster toward its final position developing increased momentum. This increased momentum could cause the motor to overshoot the final azimuth position and be forced by the system to return to the commanded position. A transient response that consists of a damped oscillation (i.e., a sinusoidal response whose amplitude diminishes with time) about the steady-state value if the gain is to high. The system's performance revolves around the transient response, steady-state error, and stability of the system.

The student will understand how a system's transfer function is found by developing each component's transfer function (see Appendix 1). The student will learn the distinguishing characteristic of an open loop system is that it cannot compensate for any disturbances that are added the system driving signal. The open-loop transfer function, damping ratio, and natural frequency were derived for the student in Appendix 2. The student will learn that the disadvantage of the open-loop system, namely sensitivity to disturbances and the inability to correct for these disturbances can be overcome by a closed-loop system (see Appendix 3).

The system transfer function is Equation (1) and the signal flow graph of the system is shown in Figure 4.

$$T(s) = \frac{6.63K}{S^3+101.71S^2+171S+6.63K} \qquad (1)$$

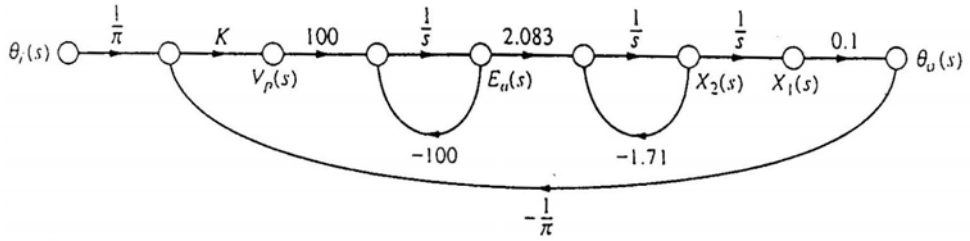

Figure 4. Signal flow graph of the azimuth position control system

The student will find that the transfer function and signal flow graph of the system were derived mathematically and verified by using Mason's gain formula[3] in Appendix 3. Also the system's state equations, damping ratio, natural frequency, peak time, settling time, percent overshoot and step response were calculated in Appendix 3. The azimuth position control system was determined to be stable for $0 < K < 2623.29$ in Appendix 4. The system was determined to be Type one and steady-state errors in response to step, ramp and parabolic functions were calculated in Appendix 5. The asymptotes and angles for the root locus were calculated in Appendix 6 and the root locus was plotted using MATLAB commercial software.[4]

Tracking Subsystem

The tracking subsystem consists of the search subsystem, the speed control system, receiver, and pedestal control box. Accuracy of the tracking subsystem depends on the accuracy of the speed control system. The motor of the speed control system rotates a 2 to 8 GHz conical spiral signal feed about the central mechanical axis of a six-foot

parabolic reflector. The reflected signal is provided to a receiver and angle data is provided to a computer. The antenna is divided into 16 sectors. Each sector is 22.5 degrees in width. The averaging of receiver automatic gain control (AGC) samples and resolution into vector components by the computer continues for each successive sector until the computations for all sectors are completed. The computer provides an azimuth and elevation drive signal to the position control system during the track mode of operation. An operator monitors the receiver signal display during the search mode of operation. When the beacon signal is detected, the operator switches the system to the track mode of operation. Thus, a stable speed control system is very important.

The subsystem uses a proportional-plus-integral (PI) compensator to improve its steady-state response. The system transfer function in Equation (2) was developed from Figure 6 by using Mason's rule.

$$T_s(s) = \frac{125}{S^3+15S^2+75S+125} \qquad (2)$$

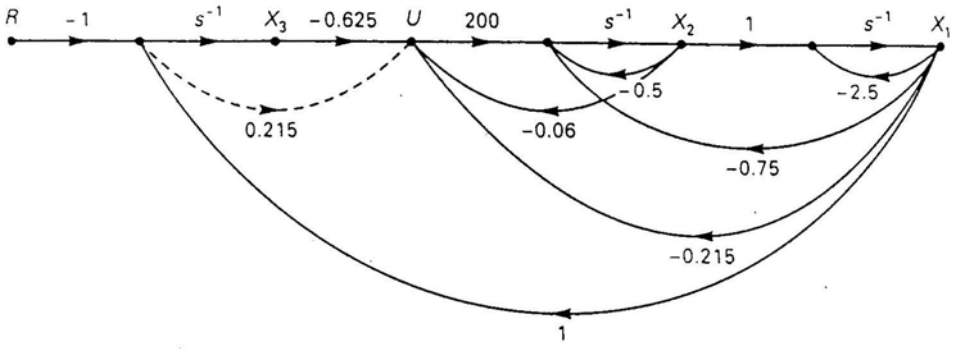

Figure 6 Signal flow graph of the speed control system.

The speed control system will be described in three parts - - motor, plant and system.

Motor

The simulation diagram for this a servomotor is shown in Figure 7.[5]

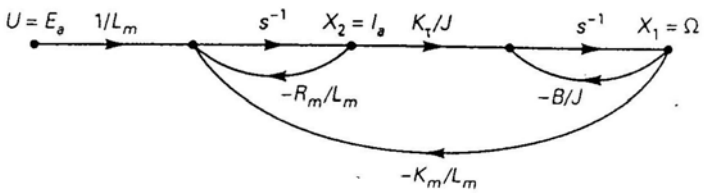

Figure 7 Signal flow diagram for a servomotor

Parameters of the servomotor and were assigned numerical values as shown in Figure 8.

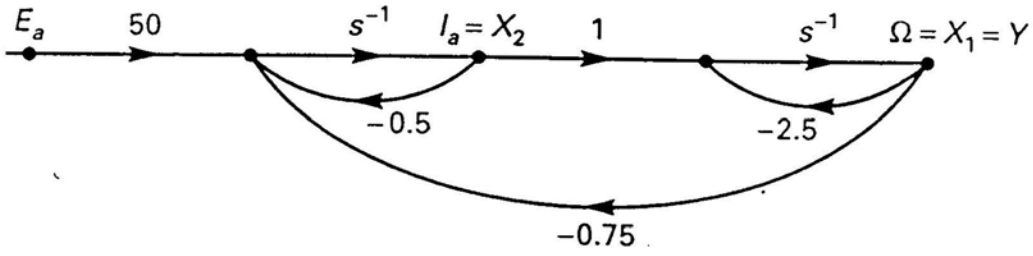

Figure 8 Servomotor and power amplifier parameters for the speed control system

The transfer function of the 24 VDC servomotor, Equation (3), was developed from Figure 8. The DC gain of the motor is 25. Therefore, the servomotor will run at a speed of 600 rpm (25x24 = 600).

$$T_m(s) = \frac{50}{(S+1)(S+2)} \qquad (3)$$

SIMULINK software was used to verify that the motor transfer function will drive the 24 VDC servomotor at 600 rpm. Figure A7.1 of Appendix 7 shows the block diagram used to run the SIMULINK program in MATLAB. Figure A7.2 shows that the servomotor will run at 600 rpm with a 24 VDC step function input.

Plant

A power amplifier was added with a gain of four. The voltage input to the amplifier is then 6 VDC. The plant transfer is the following:

$$T_p(s) = \frac{200}{(S+1)(S+2)} \qquad (4)$$

The DC gain of the plant is 100. Therefore, 6 VDC input produces 600 rpm (6x100 = 600). SIMULINK software was used to verify that the plant transfer function will drive the servomotor at 600 rpm. Figure A7.3 of Appendix 7 shows the block diagram used to run the SIMULINK program in MATLAB. Figure A7.4 shows that the servomotor will run at 600 rpm with a 6 VDC step function input.

System

A PI compensator is added to the plant. The PI compensator yields zero steady-state error for the speed control system.[6] With the PI compensator, speed resolution of the speed control system is 1 rpm. The system transfer function was shown above in Equation (2). SIMULINK software was used to verify that the system transfer function will drive the servomotor at 600 rpm. Figure A7.5 of Appendix 7 shows the block diagram used to run the SIMULINK program in MATLAB. Figure A7.6 shows that the

servomotor will run at 600 rpm with a 600 VDC step function input. The root locus of the system shown in Appendix 7 was plotted using MATLAB commercial software. Figure A7.7 shows that the speed control is a stable system.

Conclusion

The MD system described in this paper will be only one part of the proposed MD course. The student will learn how mathematical models, called transfer functions, were derived for both subsystems. These models were verified by using MATLAB commercial software which the student will exercise in the proposed MD course. The step response yields a clear picture of the system's transient response. It was found that the system gain controls the damping of the azimuth position control system. Recommend the gain of the azimuth position control system be a value between 10 and 100 to reduce overshoot.

The speed control system runs constantly at 600 rpm. The transient response is not critical for the speed control system since it does not start, stop, and go forward and backwards like the azimuth control system. A constant speed is the critical factor for the beacon tracking system to accurately track missiles. The PI compensator provides zero steady error for the speed control system. Appendices 7 shows that the system transfer function derived will drive the speed control system at 600 rpm.

The student will discover that the root locus empowers us with qualitative and quantitative information about the stability of both subsystems. The root locus of the azimuth position control system, Figure A6.1, shows that the system is stable. All roots are in the left-half of the s-plane. However, in Appendix 4, the system was determined to be stable if the system gain was $0<K<2623.9$. Figure A7.7 shows that the speed control system is also a stable system. Thus, the beacon tracking system is a stable system.

The student will find that MATLAB software provides powerful tools in the analysis of feedback control systems. SIMULINK is a MATLAB toolbox designed for the dynamic simulation of linear and nonlinear systems as well as continuous and discrete-time analysis. Parameters for these tokens are defined through user-friendly dialog boxes or by direct entry of values in graphical representations of circuit schematics.

Recommendation

Recommend an elective course covering missile defense technology be established at Universities. This course should cover subsystems needed for a ballistic missile defense engagement during powered, ballistic, and re-entry flights. A text book for the course should be written to include the design of all the subsystems needed for these engagements. This paper could be a chapter or a small part included in the textbook. Other authors could provide chapters. We should start now to develop this course because of the time needed to establish a course at a University. Graduates with this type of knowledge will be in great demand if the U.S. is attacked

by North Korean or Iranian ballistic missiles bearing nuclear or biological weapons. Presently missile defense is not considered important just like our space program was before the Soviet Union launched the Sputnik satellite. History changed on October 4, 1957, when the Soviet Union successfully launched Sputnik I. That launch ushered in new political, military, technological, and scientific developments. While the Sputnik launch was a single event, it marked the start of the space age and the U.S.-U.S.S.R space race. When the first missile destroys a USA city, this single event will mark the start of the missile defense age. This event will also usher in new political, military, technological, and scientific developments.

APPENDIX 1

AZIMUTH POSITION CONTROL SYSTEM

COMPONENT TRANSFER FUNCTION

The physical components of the azimuth position control system in Figure 1 will be modeled mathematically with transfer functions.

INPUT AND OUTPUT POTENTIOMETERS

Since the input and output potentiometers are configured the same, their transfer functions will be the same. The input potentiometer is positioned by the computer output and the output potentiometer is positioned by a small gear off the main antenna drive gear. The center position of each potentiometer outputs zero volts. The outer most position of each potentiometer is ±10 volts. Thus, the transfer function is found by the Laplace transform of the output voltage change divided by the angular displacement:

$$\frac{v_{i(s)}}{\theta_i(s)} = \frac{10}{10s} = \frac{1}{s} \qquad \text{(A1.1)}$$

where,

$v_i(s)$ is the Laplace transform of the potentiometer output voltage.

$\theta_i(s)$ is the Laplace transform of the angular displacement of the poteniometer.

PREAMPLIFIER

The transfer function of the preamplifier is given by the Laplace transform of its output voltage divided by its input voltage:

$$\frac{V_p(s)}{V_e(s)} = K \qquad \text{(A1.2)}$$

where,

$V_p(s)$ is the Laplace transform of the output voltage of the preamplifier $v_p(t)$.

$V_e(s)$ is the Laplace transform of the input difference voltage $[v_i(t) - v_o(t)]$ of the input and output poteniometers.

POWER AMPLIFIER

The transfer function of the power amplifier is given the Laplace transform of the amplifier output voltage divided by the input voltage:

$$\frac{E_a(s)}{Vp(s)} = \frac{K}{S+1} \qquad \text{(A1.3)}$$

letting $K = 100$

$$\frac{E_a(s)}{Vp(s)} = \frac{100}{S+1} \qquad \text{(A1.4)}$$

where,

$E_a(s)$ is the Laplace transform of the voltage, $e_a(t)$, to the motor.

$Vp(s)$ is the Laplace transform of the voltage, $v_p(t)$, to the power amplifier.

MOTOR AND LOAD

A motor is an electromechanical component that yields a did placement output for voltage input, that is, a mechanical output generated by an electrical input. The transfer function will derived for an armature-controlled DC servomotor. The motor schematic is shown in Figure A1.1, and the transfer function to be derived appears in figure A1.2.

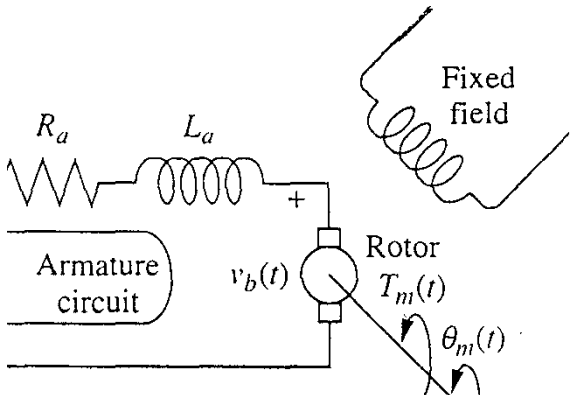

Figure A1.1. DC motor schematic.

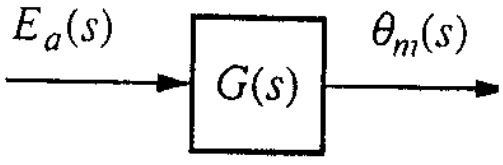

Figure A1.2. DC motor block diagram

A magnetic field is developed by a stationary electromagnet field. A rotating circuit called the armature passes through this electromagnetic field at right angles and feels a force. The resulting torque turns the motor. Since the current-carrying armature is rotating in a magnetic field, its voltage is proportional to speed: [2]

$$v_b(t) = K_b \frac{d\theta_m(t)}{dt} \tag{A1.5}$$

where,

$v_b(t)$ is the back electromotive force (back emf).

K_b is a constant of proportionality called the back emf constant.

$\frac{d\theta_m(t)}{dt}$ is the angular velocity of the motor.

taking the Laplace transform yields:

$$V_b(s) = K_b s \theta_m(s) \tag{A1.6}$$

The relationship between armature current, applied voltage and back emf is found by writing a loop equation around the Laplace transformed armature circuit in Figure A1.1.

$$R_a I_a(s) + L_a s I_a(s) + V_b(s) = E_a(s) \tag{A1.7}$$

where,

R_a is the armature resistance.

$I_a(s)$ is the Laplace transform of the armature current, $i_a(t)$.

L_a is the armature inductance.

$V_b(s)$ is the Laplace transform of the back emf, $v_b(t)$.

$E_a(s)$ is the Laplace transform of the applied armature voltage, $v_a(t)$.

The torque developed by the motor is proportional to the armature current:

therefore,

$$T_m(s) = K_t I_a(s) \tag{A1.8}$$

$$I_a(s) = \frac{T_m(s)}{K_t} \tag{A1.9}$$

where,

$T_m(s)$ is the Laplace transform of the torque developed by the motor, $t_m(t)$.

K_t is a constant of proportionality called the motor torque constant.

The transfer function of the motor is found by substituting Equations (A1.6) and (A1.9) into Equation (A1.7):

$$\frac{(R_a+L_a s)T_m(s)}{K_t} + K_b s\theta_m(s) = E_a(s) \tag{A1.10}$$

$T_m(s)$ must be expressed in terms of $\theta_m(s)$ if we are to separate the input and output variables and obtain the transfer function $\frac{\theta_m(s)}{E_a(s)}$: [2]

$$T_m(s) = (J_m s^2 + D_m s)\theta_m(s) \tag{A1.11}$$

where,

J_m is the equivalent inertia at the armature and includes both armature and load inertia reflected to the armature.

D_m is the equivalent viscus damping at the armature and includes both the armature and load viscus damping reflected to the armature.

Substituting Equations (A1.11) into Equation (A1.10) yields:

$$\frac{(R_a+L_aS)(J_mS^2+D_mS)\theta_m}{K_i} + K_bS\theta_m(s) = E_a(s) \qquad \text{(A1.12)}$$

If it is assumed that the armature induction is small compared to the armature resistance which is usual for a DC motor, Equation (A1.12) becomes:

$$[\frac{R_a}{K_i}(J_mS + D_m) + K_b]S\theta_m(s) = E_a(s) \qquad \text{(A1.13)}$$

After simplification, the desired transfer function is found to be: [2]

$$\frac{\theta_m(s)}{E_a(s)} = \frac{\frac{K_i}{R_aJ_m}}{S[S+\frac{1}{J_m}(D_m+\frac{K_iK_b}{R_a})]} \qquad \text{(A1.14)}$$

In order to use Equation (A1.14), J_m and D_m have to be defined:

$$J_m = J_a + J_L(\frac{N_1}{N_2})^2 \qquad \text{(A1.15)}$$

$$D_m = D_a + D_L\left(\frac{N_1}{N_2}\right)^2 \qquad \text{(A1.16)}$$

where,

J_a is the armature inertia.

J_L is the load inertia.

D_a is the armature damping.

D_L is the load damping.

N_1 is the armature gear.

N_2 is the load gear.

therefore,

$$J_m = 0.02 + 1\left(\frac{25}{250}\right)^2 = .03 \qquad \text{(A1.17)}$$

$$D_m = 0.01 + 1\left(\frac{25}{250}\right)^2 = .02 \qquad \text{(A1.18)}$$

Substituting J_m and D_m into Equation (A1.14) to obtain the motor transfer function:

$$\frac{\theta_0(s)}{E_a(s)} = \frac{2.083}{S(S+1.71)} \qquad \text{(A1.19)}$$

To complete the transfer function of the motor, multiply Equation (A1.19) by the gear ratio to arrive at the transfer function relating load displacement to armature voltage:

$$\frac{\theta_0(s)}{E_a(s)} = \left(\frac{25}{250}\right)\frac{2.083}{S(S+1.71)} = \frac{.2083}{S(S+1.71)} \qquad \text{(A1.20)}$$

APPENDIX 2

AZIMUTH POSITION CONTROL SYSTEM

OPEN-LOOP RESPONSE

Transfer functions of the power amplifer, motor and load being multiplied by S are shown in Figure A2.1. Differentiating the angular position of the motor and the load output by multiplying by s, gives the angular velocity ($\omega_0(s)$). The equivalent transfer function is shown in Figure A2.2. It is the product of the individual transfer functions.

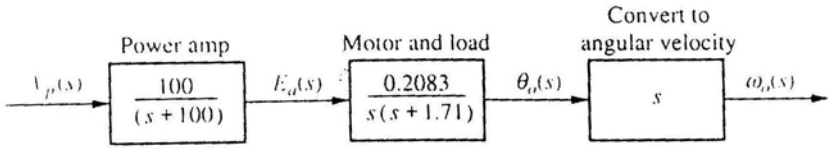

Figure A2.1. Azimuth position control system for angular velocity.

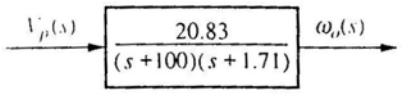

Figure A2.2. Azimuth position control system equivalent transfer function

In order to derive the angular velocity response to a step function, the transfer function In Figure A2.2 is multiplied by a step input, $\frac{1}{S}$:

$$\omega_0(s) = \frac{20.83}{S(S+100)(S+1.71)} \quad \text{(A2.1)}$$

Expanding Equation (A2.1) into partial fractions:

$$\omega_0(s) = \frac{0.122}{S} + \frac{2.12X10^{-3}}{(S+100)} - \frac{0.124}{(S+1.71)} \quad \text{(A2.2)}$$

Transforming to the time domain yields:

$$\omega_0(t) = 0.122 + (2.12X10^{-3})e^{-100t} - 0.124e^{-171t} \quad \text{(A2.3)}$$

The damping ratio and natural frequence of the open loop system can be found by expanding the denominator of the open loop transfer function shown in Figure A2.2:

$$S^2 + 101.71S + 171 \quad \text{(A2.4)}$$

$$\omega_n = \sqrt{171} = 13.08 \quad \text{(A2.5)}$$

$$2\zeta\omega_n = 101.71 \quad \text{(A2.6)}$$

$$\zeta = 3.89 \text{ (overdamped)} \quad \text{(A2.7)}$$

APPENDIX 3

AZIMUTH POSITION CONTROL SYSTEM
CLOSED-LOOP RESPONSE

COMPONENT TRANSFER FUNCTION

Substituting the transfer functions of the physical components into Figure 2, produces Figure A3.1.

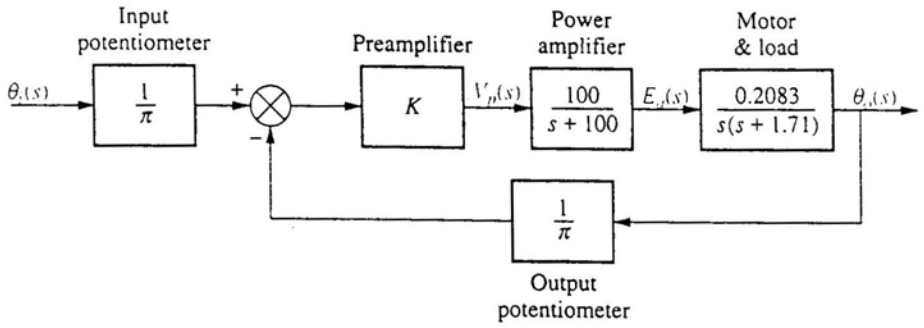

Figure A3.1. Transfer functions of physical components.

UNITY FEED BACK DIAGRAM

Converting Figure A3.1 into a unity feed back diagram produces Figure A3.2.

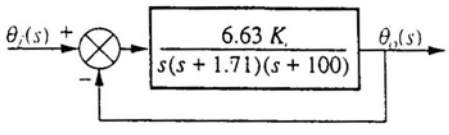

Figure A3.2. Unity feed back diagram.

CLOSED-LOOP TRANSFER FUNCTION

Converting Figure A3.2 into, $T(s) = \frac{GH}{1+GH}$, produces Figure A3.3.

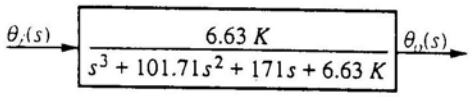

Figure A3.3. Azimuth position control system transfer function.

SIGNAL FLOW DIAGRAM

Drawing the signal flow diagram from the closed-loop transfer function shown in Figure A3.3 yields:

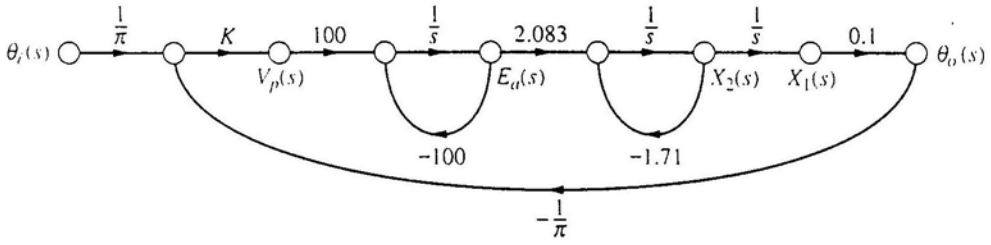

Figure A3.4. Signal flow diagram for the azimuth position control system.

STATE EQUATIONS

The stare equations can be developed from Figure A3.4 by defining the state variables as outputs of the integrators:

$$X_1' = X_2 \tag{A.3.1}$$

$$X_2' = -171\,X_2 + 2.083\,e_a \tag{A3.2}$$

$$e_a' = -3.1K\,X_1 - 100\,e_a + 31.8K\,\theta_i \tag{A3.3}$$

$$Y = \theta_0 = 0.1X_1 \tag{A3.4}$$

In matrix form:

$$X' = \begin{bmatrix} 0 & 1 & 0 \\ 0 & -1,71 & 2.083 \\ -3,18K & 0 & -100 \end{bmatrix} X + \begin{bmatrix} 0 \\ 0 \\ 31.8K \end{bmatrix} \theta_i \tag{A3.5}$$

$$Y = \begin{bmatrix} 0.1 & 0 & 0 \end{bmatrix} X \tag{A3.6}$$

Applying Mason's rule to Figure A3.4, the closed-loop transfer function shown in Figure A3.3 can be verified: [2]

$$M_1 = \frac{6.63K}{S^3} \tag{A3.7}$$

$$\Delta_1 = 1 \tag{A3.8}$$

$$\Delta = 1 + \frac{100}{S} + \frac{1.71}{S} + \frac{6.63K}{S^2} + \frac{171}{S^3} \tag{A3.9}$$

Therefore,

$$T(s) = \frac{6.63}{S^3+101,71S^2+171S+6.63K} \tag{A3.10}$$

Equation (A3.10) verifies that the transfer function shown in Figure A3.3 is the closed-loop transfer function of the azimuth position control system.

UNDAMPED SECOND ORDER SYSTEM

Replacing the power amplifier with unity gain and letting K in Figure A3.2 equal 1000 yields a forward transfer function:

$$G(s) = \frac{66.3}{S(S+1.71)} \quad \text{(A3.11)}$$

Converting to, $T(s) = \frac{G}{1+G}$,

$$T(s) = \frac{66.3}{S^2+1.71S+66.3} \quad \text{(A3.12)}$$

Thus,

$$\omega_n = \sqrt{66.3} = 8.1425 \quad \text{(A3.13)}$$

$$1.71 = 2\zeta\omega_n \quad \text{(A3.14)}$$

$$\zeta = \frac{1.71}{2\times 8.1425} = .105 \quad \text{(A3.15)}$$

where,

ω_n is the natural frequency and the frequency of oscillation of the system without damping.

ζ is the damping ratio.

PEAK TIME [2]

$$T_P = \frac{\pi}{\omega_n\sqrt{1-\zeta^2}} \quad \text{(A3.16)}$$

$$T_p = \frac{3.14}{8.14\sqrt{1-.105^2}} = .38789 \text{ seconds} \quad \text{(A3.17)}$$

where,

T_p is the time required for the transient's damped oscillation to reach and stay with in ±2% of the steady-state value.

SETTLING TIME [2]

$$T(s) = \frac{4}{\zeta\omega_n} = \frac{4}{.105\times 8.14} = 4.68 \text{ seconds} \quad \text{(A3.18)}$$

PERCENT OVERSHOOT [2]

$$\%OS = e^{-\left(\frac{\zeta\pi}{\sqrt{1-\zeta^2}}\right)} \times 100 \quad \text{(A3.19)}$$

$$\%OS = e^{-\left(\frac{.105\times 3.14}{\sqrt{1-.105^2}}\right)} \times 100 = 71.89\% \quad \text{(A3.20)}$$

where,

$\%OS$ is the amount that the waveform overshoots the steady=state value of the peak time, expressed in % of the steady state value.

STEP RESPONSE

The Laplace transform of the step response is found by multiplying $T(s)$ by $\frac{1}{S}$ and expanding to partial fractions:

$$C(s) = \frac{6.63}{S(S^2+1.71S+66.3)} = \frac{1}{S} - \frac{S+1.71}{S^2+1.71S+66.3} \quad \text{(A3.21)}$$

Using MATLAB program in Figure A3.5 the roots were calculated:

$$C(s) = \frac{1}{S} - \frac{(S+0.855)+0.106(8.097)}{(S+.855)^2+(8.097)^2} \quad \text{(A3.22)}$$

Taking the inverse Laplace transform:

$$C(t) = 1 - e^{-0.855t}(\cos 8.097t + 0.106 \sin 8.097) \qquad \text{(A3.23)}$$

```
»
» p=[1 1.71 66.3];
» roots(p)

ans =

  -0.8550 + 8.0975i
  -0.8550 - 8.0975i
```

Figure A3.5. MATLAB program roots.

APPENDIX 4

AZIMUTH POSITION CONTROL SYSTEM STABILITY

Stable systems have their closed-loop poles in the left-half of the s-plane. As the loop gain is changed, the location of the poles are also changed. They could move to the right-half of the s-plane, which yields instability. Proper gain settings are essential for the stability of closed loop systems. The Routh-Hurwitz stability criterion will be used to determine the stability of this system. [1]

ROUTH-HUNWITZ STABILITY CRITERION

The closed-loop transfer function developed in Appendix 3 is shown below:

$$T(s) = \frac{6.63K}{S^3+101.71S^2+171S+6.63K} \qquad \text{(A4.1)}$$

Using the denominator, the Routh-Hurwity table is developed: [2]

S^3	1	171.0
S^2	101.71	$6.63K$
S^1	$17392.41 - 6.63K$	0
S^0	$6.63K$	0

Table A4.I. Routh-Hurwity table for the azimuth position control system.

The third row of Table A4.1 shows that a row of zeros occurs if $K = 2623.29$. This value makes the system marginally stable. There will be no sign change in the first column if $0 < K < 2623.29$. Therefore, the system is stable for $0 < K < 2623.29$.

APPENDIX 5

AZIMUTH POSITION CONTROL SYSTEM

STEADY-STATE ERRORS

Steady-state error is the difference between the input and output for a prescribed test input at $t \rightarrow \infty$. Step inputs represent constant position and are useful in determining the ability of the a position control system to position itself with respect to a stationary target. Ramp inputs represent constant velocity input to a position control system by their linearly increasing amplitude. The parabola represents constant acceleration input to the position control system and can be used to represent accelerating targets. These waveforms can be used to test the position control system's ability to track missiles. The steady-state error is given by: [4]

$$e(\infty) = \underset{s \rightarrow 0}{Lim}\, sE(s) = \underset{s \rightarrow 0}{Lim}\, \frac{sR(s)}{1+G(s)} \qquad \text{(A5.1)}$$

From Equation (A3.3):

$$G(s) = \frac{6.63K}{S(S+1.71)(S+100)} \qquad \text{(A5.2)}$$

STEP FUNCTION

Substituting Equation (A5.2) and $R(s) = \frac{1}{S}$:

$$e(\infty) =_s \underset{\to 0}{Lim} = \frac{S(\frac{1}{S})}{1+\frac{6.63K}{S(S+1.71)(S+100)}} = 0 \qquad \text{(A5.3)}$$

RAMP FUNCTION

Substituting Equation (A5.2) and $R(s) = \frac{1}{s^2}$:

$$e(\infty) =_s \underset{\to 0}{Lim} = \frac{S(\frac{1}{s^2})}{1+\frac{6.63K}{S(S+1.71)(S+100)}} = \frac{25.79}{k} \qquad \text{(A5.4)}$$

Parabolic function

Substituting Equation (A5.2) and $R(s) = \frac{1}{S^3}$:

$$e(\infty) =_s \underset{\to 0}{Lim} = \frac{S(\frac{1}{s^3})}{1+\frac{6.63K}{S(S+1.71)(S+100)}} = \infty \qquad \text{(A5.5)}$$

SYSTEM TYPE

Since the system is Type 1, a 10 % error in the steady-state must refer to a ramp function. This is the only input that yeilds a finite, nonzero error.

Therefore, for a unit ramp function: [1]

$$e(\infty) = 0.1 = \frac{25.79}{K} \qquad \text{(A5.6)}$$

$$K = \frac{25.79}{0.1} = 257.9 \qquad \text{(A5.7)}$$

The system is stabile for a gain of 257.9 because the range of gain for stability was found in Appendix 4 to be $0 < K < 2623.29$.

APPENDIX 6

AZIMUTH POSITION CONTROL SYSTEM

ROOT LOCUS

The forward transfer function was found in Appendix 3 to be:

$$G(s) = \frac{6.63K}{S(S+1.71)(S+100)} \tag{A6.1}$$

ASYMPTOTES

The asymptotes of this function are calculated by: [2]

$$\sigma = \frac{\sum \text{finite poles} - \sum \text{finite zeros}}{\#\text{finite poles} - \#\text{finite zeros}} \tag{A6.2}$$

$$\sigma = \frac{-101.71-0}{3-0} = -33.903 \tag{A6.3}$$

ANGLES

Angles of this function are calculated by: [2]

$$\theta = \frac{(2K+1)\pi}{\#\text{finite poles} - \#\text{finite zeros}} \tag{A6.4}$$

$$\theta = \frac{(2K+1)\pi}{3}\left(\frac{180}{\pi}\right) \tag{A6.5}$$

For $K = 0, \pm 1$

$$\theta_0 = \frac{\pi}{3}\left(\frac{180^0}{\pi}\right) = 60^0 \tag{A6.6}$$

$$\theta_0 = \frac{3\pi}{3}\left(\frac{180^0}{\pi}\right) = 180^0 \tag{A6.7}$$

$$\theta_0 = -\frac{\pi}{3}\left(\frac{180^0}{\pi}\right) = -60^0 \tag{A6.8}$$

The real-axis segments are found to be between the origin and -171.1, and from -100. The locus begins at the open-loop poles, which are all on the real-axis at -33.903 at angles 60, 180, and -60. Table A6.I is the MATLAB program to plot the root locus. The plot of the root locus is shown in Figure A6.1.

```
»
»
»
»
»
»
» p=[1 101.71 171 6.63];
» roots(p)

ans =

 -100.0007
   -1.6696
   -0.0397

» gnum=[0 0 0 6.63];
» gden=[1 101.71 171 6.63];
» rlocus(gnum,gden)
»
»
» title('Figure A6-1. Root Locus of Azimuth Position Control System')
```

Table A6.I MATLAB Program for Root Locus of Azimuth position Control System

Figure A6-1. Root Locus of Azimuth Position Control System

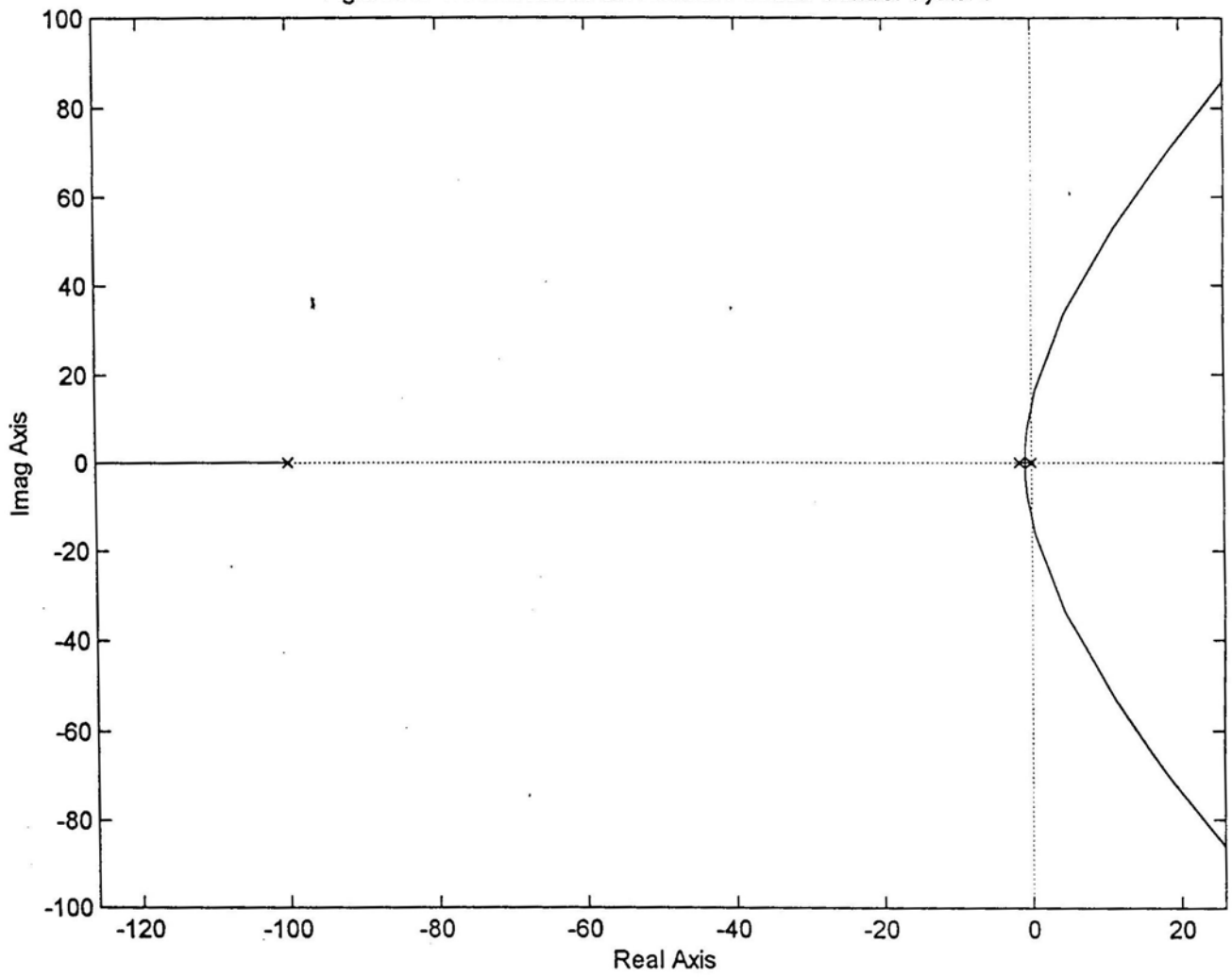

APPENDIX 7
SPEED CONTROL SYSTEM

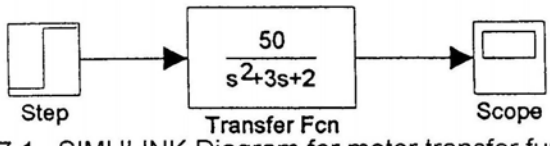

Figure A7.1. SIMULINK Diagram for motor transfer function.

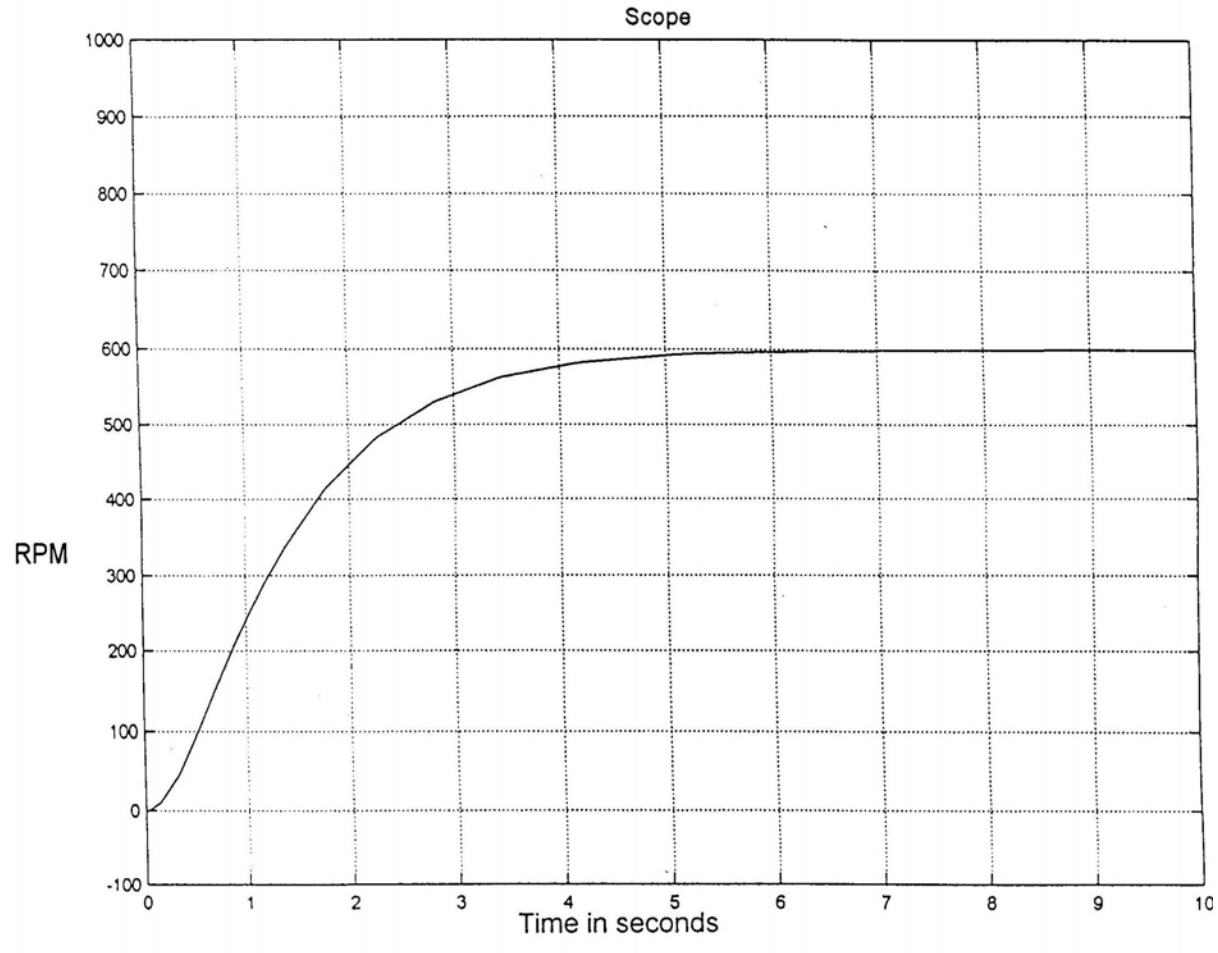

Figure A7.2. 24 VDC Step response for motor transfer function

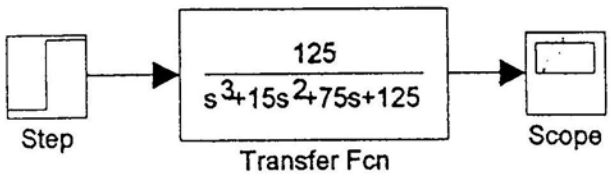

Figure A7.5. SIMULINK Diagram for system transfer function.

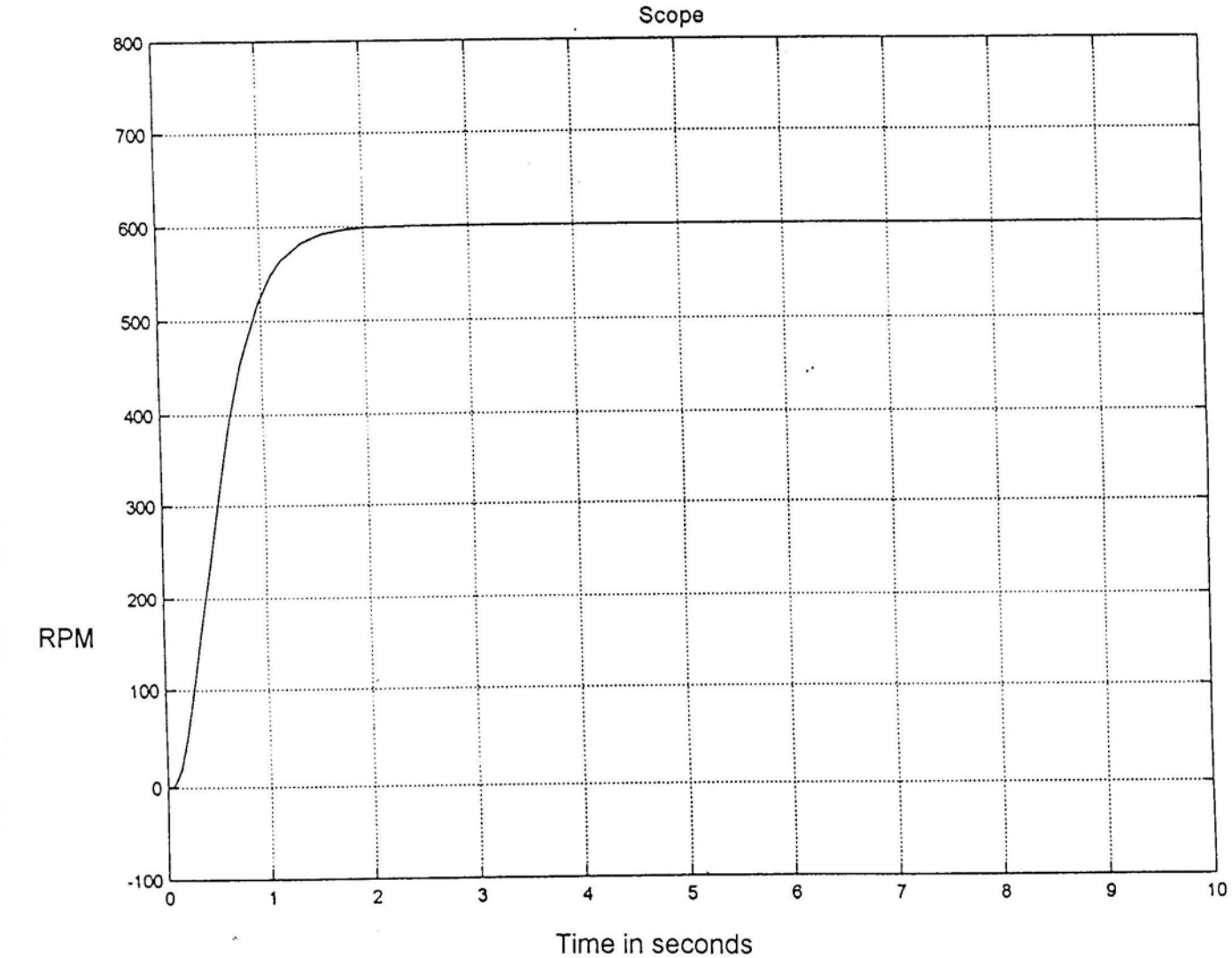

Figure A7.6. RPM Step response for system transfer function,
(Step input equals RPM)

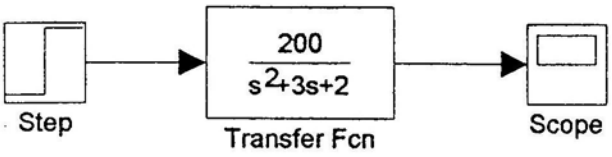

Figure A7.3. SIMULINK Diagram for plant transfer function.

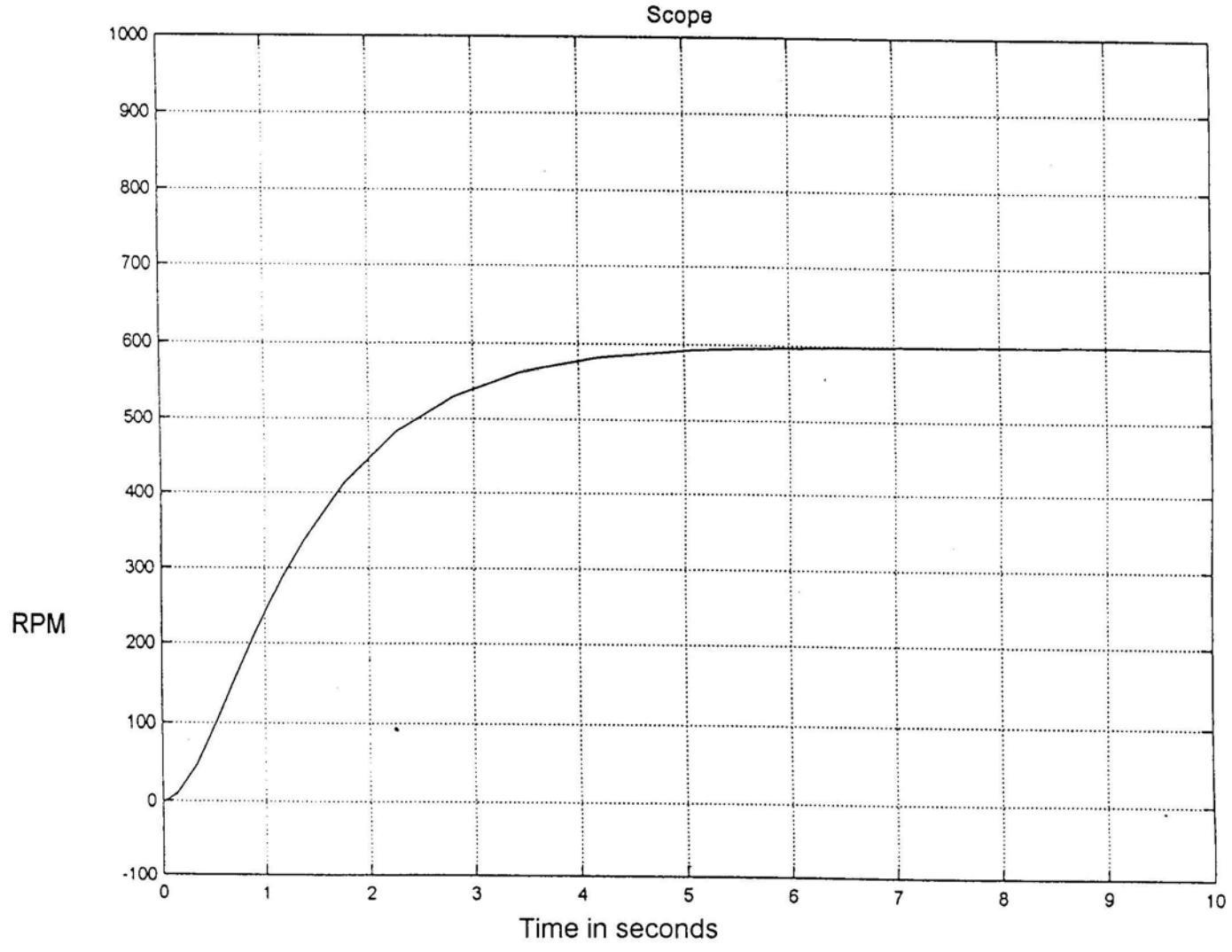

Figure A7.4. 6 VDC Step response for plant transfer function

```
»
»
»
»
»
»
» p=[1 15 75 125];
» roots(p)

ans =

  -5.0000 + 0.0000i
  -5.0000 - 0.0000i
  -5.0000

» gnum=[0 0 0 125];
» gden=[1 15 75 125];
» rlocus(gnum,gden)


» title('Figure A7.7 Root locus of speed control system.')
```

Table A7.1 MATLAB program for Root Locus of speed control system.

Figure A7.7 Root locus of speed control system.

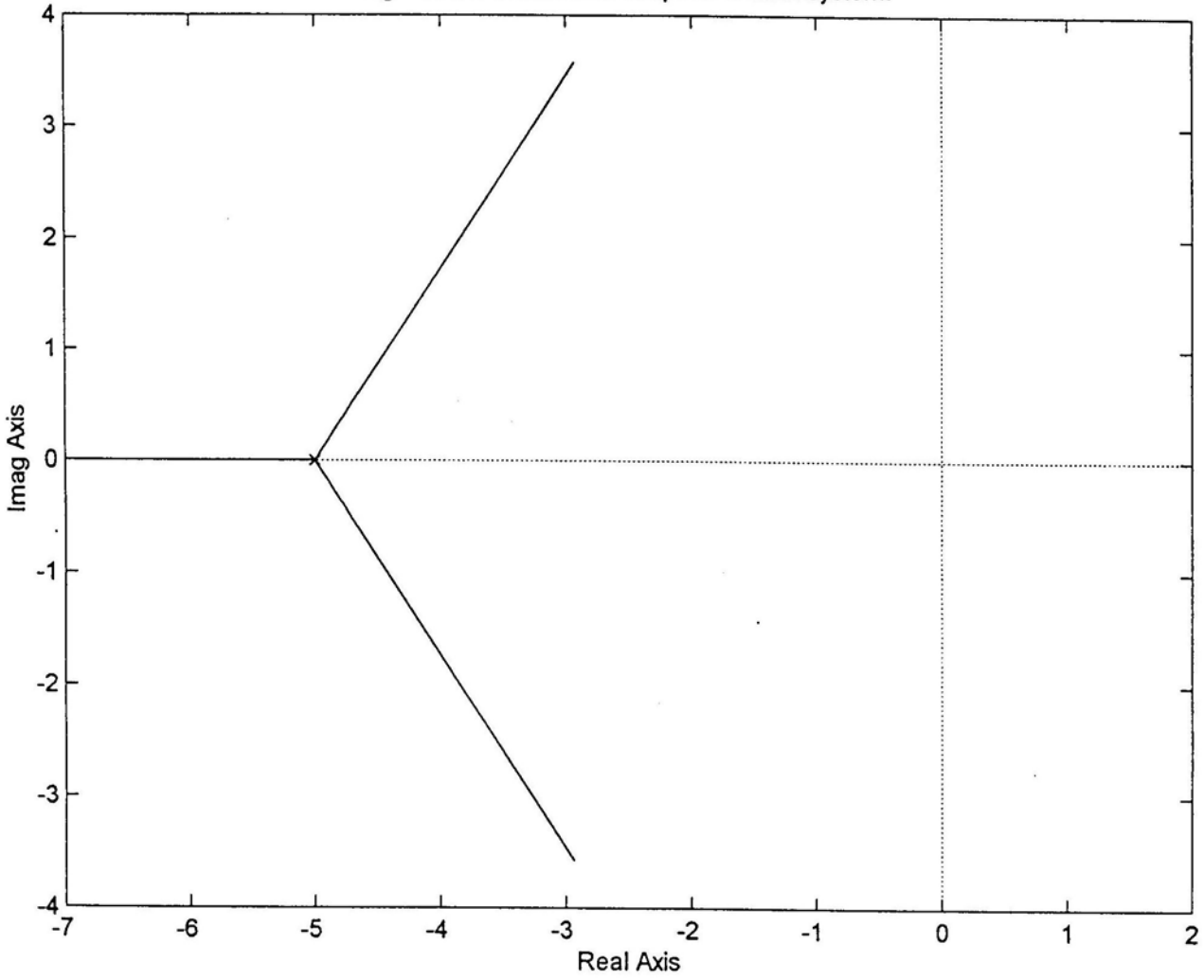

REFERENCE

1. Burgess E., *Long-Range Ballistic Missiles*, The Macmillan Company, New York, NY, p 58, 1961.
2. C. C Bittle and M. C. Plummer, *A Statistical Method, using LabVIEW® Software, To Determine Missile Defense System Locations,* Presented at the 2007 ASEE Annual Conference & Exposition, June 23-27, Hawaii.
3. C. L. Phillips, H. T. Nagle, *Digital Control System Analysis and Design,* Prentice Hall, Inc., Englewood Cliffs, N. J., pp. 532,1984.
4. A. Cavallo, R. Setola, F. Vasca, *Using MATLAB, Simulink and control System Toolbox*, Prentice Hall Europe, London, 1996.
5. C. L. Phillips, R. D. Harbor, *Feedback Control Systems*, Third Edition, Prentice Hall, Inc., Upper Saddle River, New Jersey, pp. 369-400, 1996.
6. W. S. Levine, *The Control Handbook*, CRC Press, Inc., Boca Raton, Florida, pp.1393,1996.